PHYSICAL REVIEW D VOLUME 48, NUMBER 3 1 AUGUST 1993

Masses of vector and axial-vector mesons at finite temperature

Chungsik Song
School of Physics and Astronomy, University of Minnesota, Minneapolis, Minnesota 55455
(Received 15 January 1993)

The temperature dependence of the effective masses of vector mesons (ρ and ω) and axial-vector mesons (A_1) are examined with the use of an effective chiral Lagrangian. The effective masses at finite temperature are determined from the pole positions of the propagators and from the inverses of the static screening lengths. The results may be viewed as an extrapolation of known hadronic interactions to temperatures up to a deconfinement/chiral-symmetry-restoring transition or crossover.

PACS number(s): 12.38.Mh, 11.30.Rd, 12.40.Vv, 14.40.Cs

I. INTRODUCTION

We believe that the fundamental theory of the strong interactions is quantum chromodynamics (QCD) with quarks and gluons as the elementary fields. If the quark masses are set equal to zero, the QCD Lagrangian is symmetric under the chiral group $SU(N_f)\times SU(N_f)$. Since the u- and d-quark masses are very small, this is a good approximation for the subgroup $SU(2)\times SU(2)$.

In the hadronic phase, at low energy, quarks and gluons are confined in hadrons: pions, nucleons, vector mesons, and others. Since each hadron does not have the parity-doubled partner, one assumes that the ground state of the theory spontaneously breaks the chiral symmetry down to $SU(N_f)$. Spontaneous breaking of the symmetry is accompanied by the appearance of N_f^2-1 massless Goldstone bosons. Pions, kaons, and η mesons are regarded as these Goldstone bosons.

As the energy density of the hadronic system increases, it is expected that the system undergoes a phase transition and/or crossover to a quark-gluon plasma (QGP) [1–3] in which quarks and gluons are deconfined and the spontaneously broken symmetry is restored. Thus there are at least two possible phase transitions in hadronic matter as temperature increases: deconfinement of quarks and gluons at temperature T_d and restoration of the broken chiral symmetry at temperature $T_{\rm ch}$ [4,5]. These phase transitions are very important to understand QCD and the QGP phase at high temperature.

By studying the properties of hadrons at finite temperature we may be able to understand the approach to the expected phase transitions and/or crossover and the formation of the new phase. The masses of the mesons are regarded as one way we can see the properties of hadronic matter. Recently, there have been estimates made of the meson masses at finite temperature by using lattice simulation [6,7], QCD sum rules [8,9], and effective Lagrangians [10].

In lattice calculations, screening masses of mesons, related to the imaginary-time response function, are measured to study the structure of the hot matter. It has been suggested that the unbroken chiral symmetries are reflected by the degeneracies of the screening masses of the expected chiral multiplets [6]. Recent Monte Carlo simulations on the lattice showed that the screening masses of the π meson and σ meson, and the ρ meson and A_1 meson, are degenerate and approach $2\pi T$, the limit which corresponds to the free-quark contribution at high temperature ($T > T_{\rm ch}$). The degeneracies are interpreted as the signals of chiral-symmetry restoration. However, there is no general proof that the screening masses are directly related to the masses of low-lying excitations in hot matter.

The calculation using QCD sum rules showed that the mass of the ρ meson increases with temperature and approaches the mass of the A_1 meson, which decreases as temperature increases [8]. Chiral-symmetry restoration was inferred from the degeneracy of the vector and axial-vector meson masses. But other calculations [9], which used a different Lorentz structure for the sum rule, showed that both vector and axial-vector meson masses decrease as temperature increases. These are supported by an argument based on scale invariance, in which all meson masses approach zero as the temperature approaches its critical value [11]. However, the mass difference between these mesons becomes even bigger as temperature increases because the ρ-meson mass decreases faster than that of the A_1 meson.

Gale and Kapusta [10] investigated the properties of the neutral ρ meson at finite temperature using an effective, renormalizable Lagrangian with charged pions and neutral ρ mesons. They found that the neutral ρ-meson mass increased slightly with temperature.

We see that there are some contradictions in the published results using different techniques. Why? First of all, there is as yet no systematic way to describe hot hadronic matter. Even though QCD is the fundamental theory, hadronic systems cannot be easily described by QCD because of confinement of elementary fields and the symmetry breaking. Another problem in estimating the masses of the mesons at finite temperature is the ambiguity of the definition of the mass [12]. Generally, different definitions describe physically different phenomena.

In this paper the vector and axial-vector meson masses are investigated and analyzed at finite temperature. We use an effective chiral Lagrangian with pions, ρ mesons,

ω mesons, and A_1 mesons. The vector and axial-vector mesons can be included in the effective Lagrangian explicitly, being regarded as massive Yang-Mills fields of the chiral symmetry which is spontaneously broken in the hadronic phase. This effective Lagrangian can describe all of the interactions in terms of a relatively small number of parameters which can be obtained phenomenologically.

The effective Lagrangian assumes confinement and spontaneous breaking of the chiral symmetry. The Lagrangian is applicable only to low temperature before the expected phase transitions. The results obtained from this approach should be viewed as valid at low temperature, and extrapolations to $T = 150$–200 MeV can be viewed only as suggestive.

In the effective Lagrangian approach, it is assumed that the properties of the system are describable at the tree level, where the masses and coupling constants are to be regarded as the physical ones. Loop diagrams, which are neglected, produce only renormalization effects on these parameters [13]. We assume that the tree approximation is still reasonable at finite temperature due to the relatively low density of the system. At finite temperature the tree-level contributions are obtained from the one-loop diagrams which are interpreted as the scattering processes in the medium [14].

We consider two definitions of the mass at finite temperature: the pole mass determined from the pole positions of the propagators [15] and the screening mass obtained from the hadronic correlation function at large spatial separation [6]. Both definitions are well known from many-body theory and are relevant in different physical contexts.

In Sec. II the effective Lagrangian used in the present calculation is described. We restrict ourselves to the $SU(2)\times SU(2)\times U(1)$ subgroup in which the ρ, ω, and A_1 mesons are included as gauge fields. Anomalous interactions are included in the effective Lagrangian by the gauged Wess-Zumino terms [16,17].

In Sec. III the effective masses of the ρ meson, ω meson, and A_1 meson are calculated from the pole positions of the propagators at finite temperature. The propagator in the medium can be obtained from the Dyson-Schwinger equation in terms of the bare propagator and the self-energy. The self-energy of the vector and axial-vector mesons are computed at the lowest order. The effective mass can be obtained from the proper limit of the components of the self-energy.

In field theory at finite temperature the screening mass can be obtained from the static limit of the time-time component of the self-energy [1]. We calculate the screening masses of these mesons in Sec. IV. The computed screening masses are compared with the effective masses from Sec. III. The electric screening mass, which is defined as the inverse Debye screening length, is obtained by introducing electromagnetic interactions in the effective Lagrangian.

In Sec. V the results are analyzed and related to the properties of the hadronic matter at finite temperature. Some useful relations are given in Appendix A, and explicit expressions for the self-energy of the ρ meson, ω meson, and A_1 meson are presented in Appendixes B, C, and D, respectively.

II. EFFECTIVE CHIRAL LAGRANGIAN

In the low-temperature hadronic phase quarks and gluons are confined, and so the system may be adequately described by a theory in which hadrons are used as elementary fields. Effective Lagrangians which preserve the chiral symmetry have been widely used and lead to successful predictions in low-energy hadron physics. This method is based on the symmetry and the vacuum structure of the fundamental theory [18–23].

At low temperature, one can work with the nonet of light pseudoscalar mesons, which are regarded as Goldstone bosons related to spontaneous breaking of chiral symmetry. These pseudoscalar mesons ϕ are related to a field U defined by

$$U = \exp\left[\frac{2i}{F_\pi}\sum_i \frac{\phi_i\lambda_i}{\sqrt{2}}\right] \equiv \exp\left[\frac{2i}{F_\pi}\phi\right], \tag{1}$$

and their interactions are described by the nonlinear σ model [20]

$$\mathcal{L}_0 = \tfrac{1}{8}F_\pi^2 \mathrm{Tr}[\partial^\mu U \partial_\mu U^\dagger], \tag{2}$$

where $F_\pi \approx 135$ MeV is the pion decay constant and the λ's are Gell-Mann matrices. We can add a chiral-symmetry-breaking term which is proportional to the masses of the Goldstone bosons:

$$\mathrm{Tr}[M(U + U^\dagger)], \tag{3}$$

where

$$M = \frac{2}{3}\left(m_k^2 + \frac{1}{2}m_\pi^2\right)\mathbb{1} - \frac{2}{\sqrt{3}}(m_k^2 - m_\pi^2)\lambda_8. \tag{4}$$

As temperature increases, we need to include the vector and axial-vector mesons. This could be done explicitly, or it could be done implicitly by including higher-order interaction terms of the pseudoscalar fields. These two approaches are nearly identical [24,25]. There is a traditional way of describing the massive spin-1 mesons at low energy in the effective chiral Lagrangian, which is based on the old notion of vector-meson dominance [18,21–23]. Those mesons are included as massive Yang-Mills-type fields of the chiral symmetry. It is convenient to introduce the left-handed vector fields A_L and right-handed vector fields A_R, which are related to the vector and axial-vector fields as

$$A_L^\mu = \tfrac{1}{2}(V^\mu + A^\mu), \tag{5}$$

$$A_R^\mu = \tfrac{1}{2}(V^\mu - A^\mu). \tag{6}$$

Equation (2) can be made gauge invariant in the presence of the gauge fields when we introduce the covariant derivative D^μ defined by

$$D^\mu U = \partial^\mu U - ig_0 A_L^\mu U + ig_0 U A_R^\mu, \tag{7}$$

where g_0 is the phenomenological gauge coupling constant. The effective Lagrangian then consists of the nonlinear σ term with a covariant derivative and kinetic terms of the spin-1 gauge fields:

$$\mathcal{L}_0 = \tfrac{1}{8}F_\pi^2\mathrm{Tr}[D_\mu U D^\mu U^\dagger] + \tfrac{1}{8}F_\pi^2\mathrm{Tr}[M(U+U^\dagger-2)] - \tfrac{1}{2}\mathrm{Tr}[F^L_{\mu\nu}F^{L\mu\nu} + F^R_{\mu\nu}F^{R\mu\nu}] + m_0^2\mathrm{Tr}[A^L_\mu A^{L\mu} + A^R_\mu A^{R\mu}], \quad (8)$$

where

$$F^{L,R}_{\mu\nu} = \partial_\mu A^{L,R}_\nu - \partial_\nu A^{L,R}_\mu - ig_0[A^{L,R}_\mu, A^{L,R}_\nu]. \quad (9)$$

We include the degenerate spin-1 mass term m_0, which breaks gauge invariance but not chiral invariance. Mass splitting is generated by the partial Higgs mechanism.

We add two more nonminimal, but gauge-invariant, coupling terms to reproduce the experimental results [26,27]

$$\mathcal{L}_{\mathrm{non}} = -i\xi\mathrm{Tr}[D_\mu U D_\nu U^\dagger F^{L\mu\nu} + D_\mu U^\dagger D_\nu U F^{R\mu\nu}] + \sigma\mathrm{Tr}[F^L_{\mu\nu}UF^{R\mu\nu}U^\dagger], \quad (10)$$

where ξ and σ are parameters to be determined.

There are anomalous interaction terms included in the effective Lagrangian, called Wess-Zumino terms, which describe the non-Abelian anomaly structure of QCD. The general structure of these anomalous terms in an arbitrary subgroup of SU(3)×SU(3) are given in Ref. [16]. We consider ρ mesons, ω mesons, and A_1 mesons which can be regarded as gauge bosons of the $\mathrm{SU}(2)_L\times\mathrm{SU}(2)_R\times\mathrm{U}(1)_V$ symmetry. The left-handed A^μ_L and right-handed A^μ_R vector fields are related to the ρ meson, ω meson, and A_1 meson as

$$A^\mu_L = \tfrac{1}{2}(\rho^\mu + \omega^\mu + A_1^\mu), \quad (11)$$

$$A^\mu_R = \tfrac{1}{2}(\rho^\mu + \omega^\mu - A_1^\mu), \quad (12)$$

with $\rho^\mu = \rho^\mu_a\tau^a/\sqrt{2}$, $\omega^\mu = \omega^\mu\mathbb{1}$, $A_1^\mu = A^\mu_{1a}\tau^a/\sqrt{2}$, and the τ_a's are the Pauli matrices. The gauged Wess-Zumino terms are [28]

$$\mathcal{L}_{\mathrm{WZ}} = -\frac{g_0N_C}{48\pi^2}\epsilon^{\mu\nu\alpha\beta}\omega_\mu\mathrm{Tr}[L_\nu L_\alpha L_\beta] - \frac{ig_0^2N_C}{16\pi^2}\epsilon^{\mu\nu\alpha\beta}\omega_\mu\partial_\nu\mathrm{Tr}[A_{R\alpha}L_\beta - A_{L\alpha}R_\beta + ig_0(A_{R\alpha}U^\dagger A_{L\beta}U - A_{R\alpha}A_{L\beta})], \quad (13)$$

where N_C is the number of colors, $\epsilon^{\mu\nu\alpha\beta}$ is the antisymmetric Levi-Civita tensor with $\epsilon^{0123}=1$, and L_α and R_α are the left and right Sugawara currents:

$$L_\alpha = U^\dagger\partial_\alpha U, \qquad R_\alpha = U\partial_\alpha U^\dagger. \quad (14)$$

The ω meson interacts with the pion and ρ meson through anomalous terms:

$$\mathcal{L}_{\omega\pi\rho} = -\frac{3g^2}{8\pi^2F_\pi}\epsilon^{\mu\nu\alpha\beta}\partial_\mu\omega_\nu\mathrm{Tr}[\partial_\alpha\rho_\beta\phi], \quad (15)$$

where

$$g = g_0/\sqrt{1-\sigma}. \quad (16)$$

When we include the electromagnetic interaction in the effective Lagrangian as [29]

$$\mathcal{L}_{\mathrm{EM}} = -\frac{\sqrt{2}e}{g}a^\mu\left(m_\rho^2\rho^0_\mu + \frac{1}{3}m_\omega^2\omega_\mu - \frac{\sqrt{2}}{3}m_\phi^2\phi_\mu\right) + \mathcal{O}(a_\mu^2), \quad (17)$$

we have

$$\Gamma(\pi^0\to\gamma\gamma) = \frac{\alpha^2}{32\pi^3}\frac{m_\pi^3}{F_\pi^3}, \quad (18)$$

which is the same as the current-algebra prediction.

As a result the Lagrangian is the sum of three terms:

$$\mathcal{L} = \mathcal{L}_0 + \mathcal{L}_{\mathrm{non}} + \mathcal{L}_{\mathrm{WZ}}. \quad (19)$$

The Lagrangian has four parameters (m_0, g, σ, ξ) which can be inferred from comparison with experimental data. We use the masses and decay widths of the ρ meson and A_1 meson to determine the parameters. When we use [30]

$$m_\rho = 768\,\mathrm{MeV}, \quad \Gamma_\rho = 149\,\mathrm{MeV}, \quad m_{A_1} = 1260\,\mathrm{MeV}, \quad \Gamma_{A_1} = 400\,\mathrm{MeV}, \quad (20)$$

we get two sets of parameters [29]:

$$\text{set I: } g = 10.3063,\ \sigma = 0.3405,\ \xi = 0.4473; \quad (21)$$

$$\text{set II: } g = 6.4483,\ \sigma = -0.2913,\ \xi = 0.0585. \quad (22)$$

Recent calculation shows that parameter set I is consistent with QCD sum-rule results [31]. We will consider both sets in what follows, but we prefer parameter set I.

III. POLE MASS

The propagator of a vector field at finite temperature ($T = 1/\beta$) is defined by [1,32]

$$i\mathcal{D}_{\mu\nu} = \langle \mathrm{T}A_\mu(x)A_\nu(0)\rangle = \mathcal{Z}^{-1}\mathrm{Tr}\{\mathrm{T}[A_\mu(x)A_\nu(0)]\exp(-\beta H)\}, \quad (23)$$

where H is the Hamiltonian and $\mathcal{Z}$ is the partition function:

$$\mathcal{Z} = \mathrm{Tr}[\exp(-\beta H)]. \quad (24)$$

Propagation of the field in the medium is modified by the interactions, and this modification can be included in the self-energy, which is related to the inverses of the full and bare propagators by

$$\Pi_{\mu\nu} = \mathcal{D}^{-1}_{\mu\nu} - \mathcal{D}^{-1}_{0\mu\nu}. \quad (25)$$

The poles of the full propagator are interpreted as the elementary excitations in the interacting system [15]. The effective masses of the elementary excitations are defined as the positions of these poles.

The propagator and the self-energy of the vector fields are symmetric second-rank tensors. We have four independent tensors at finite temperature which can be constructed from the four-momentum k_μ and the four-velocity of the heat bath n_μ, where $n_\mu = (1,0,0,0)$ in the rest frame of the heat bath. It is convenient to introduce four covariant tensors as follows [32,33]:

$$
\begin{aligned}
A_{\mu\nu} &= g_{\mu\nu} - \frac{1}{\mathbf{k}^2}[k_0(n_\mu k_\nu + n_\nu k_\mu) - k_\mu k_\nu - k^2 n_\mu n_\mu], \\
B_{\mu\nu} &= -\frac{k^2}{\mathbf{k}^2}\left(n_\mu - \frac{k_0 k_\mu}{k^2}\right)\left(n_\nu - \frac{k_0 k_\nu}{k^2}\right), \\
C_{\mu\nu} &= -\frac{1}{\sqrt{2}|\mathbf{k}|}\left[\left(n_\mu - \frac{k_0 k_\mu}{k^2}\right)k_\nu + \left(n_\nu - \frac{k_0 k_\nu}{k^2}\right)k_\mu\right], \\
D_{\mu\nu} &= \frac{k_\mu k_\nu}{k^2},
\end{aligned}
\tag{26}
$$

where $k^2 = k_0^2 - \mathbf{k}^2$. The self-energy can be written as a linear combination of these four tensors:

$$
\Pi_{\mu\nu} = \alpha A_{\mu\nu} + \beta B_{\mu\nu} + \gamma C_{\mu\nu} + \delta D_{\mu\nu}, \tag{27}
$$

where the α, β, γ, and δ are scalar functions which depend on k^2 and $k \cdot n$.

The ρ-meson self-energy has been calculated at the one-loop level (Fig. 1), and the results are given in Appendix B. The ρ-meson self-energy is transverse ($k^\mu \Pi^\rho_{\mu\nu} = 0$). In this case γ and δ vanish and there is a simple expression for the self-energy as

$$
\Pi^{\mu\nu} = G P_T^{\mu\nu} + F P_L^{\mu\nu}, \tag{28}
$$

where $P_T^{\mu\nu}$ and $P_L^{\mu\nu}$ are projection tensors defined as

$$
\begin{aligned}
P_T^{00} &= P_T^{0i} = P_T^{i0} = 0, \\
P_T^{ij} &= \delta^{ij} - k^i k^j/\mathbf{k}^2, \\
P_L^{\mu\nu} &= k^\mu k^\nu/k^2 - g^{\mu\nu} - P_T^{\mu\nu}.
\end{aligned}
\tag{29}
$$

F and G are related to the components of the self-energy by

$$
F = -\frac{k^2}{\mathbf{k}^2}\Pi_{00}, \tag{30}
$$

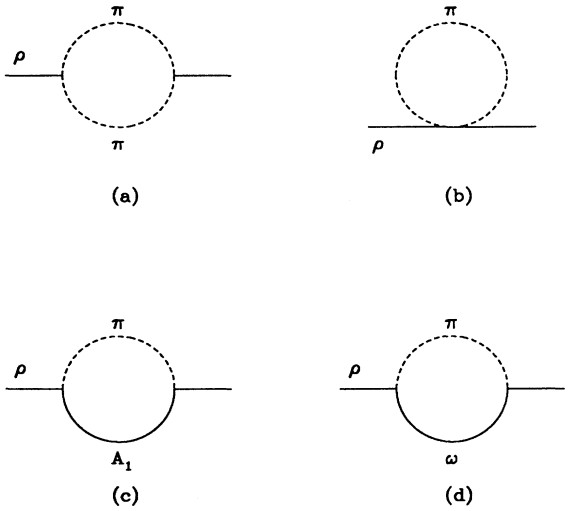

FIG. 1. One-loop contributions to the ρ-meson self-energy.

$$
G = \frac{1}{2}\left(\Pi^\mu_\mu + \frac{k^2}{\mathbf{k}^2}\Pi_{00}\right) = \frac{1}{2}\left(\Pi^i_i + \frac{k_0^2}{\mathbf{k}^2}\Pi_{00}\right). \tag{31}
$$

From Eqs. (25) and (28) the propagator of the ρ meson can be written as

$$
\mathcal{D}^{\mu\nu} = -\frac{P_L^{\mu\nu}}{k^2 - m_\rho^2 - F_\rho} - \frac{P_T^{\mu\nu}}{k^2 - m_\rho^2 - G_\rho} - \frac{k^\mu k^\nu}{m_\rho^2 k^2}. \tag{32}
$$

The poles of the propagator are determined from the equations $k^2 - m_\rho^2 - G_\rho = 0$ and $k^2 - m_\rho^2 - F_\rho = 0$, which represent the transversal and longitudinal collective excitations, respectively. In the limit where the magnitude of the spatial momentum goes to zero ($\mathbf{k} \to 0$), there is no distinction between the transversal and longitudinal motions, and so $F_\rho(k_0, \mathbf{k} \to 0)$ should be the same as $G_\rho(k_0, \mathbf{k} \to 0)$. We can define the effective mass of the ρ meson as the k_0 which satisfies the equation

$$
k_0^2 - m_\rho^2 - F_\rho(k_0, \mathbf{k} \to 0) = 0, \tag{33}
$$

where m_ρ is the vacuum mass.

In the limit $\mathbf{k} \to 0$ we obtain (see Appendixes A and B)

$$
\begin{aligned}
F_\rho(k_0, \mathbf{k} \to 0) &= G_\rho(k_0, \mathbf{k} \to 0) \\
&= g^2 \int \frac{p^2 dp}{(2\pi)^2}\left\{\frac{n(\omega_\pi)}{\omega_\pi}\left[B_1 + \frac{B_2 p^2}{(k_0^2 - 4\omega_\pi^2)} + \frac{B_3 + B_4 p^2}{(k_0^2 - m_{A_1}^2 + m_\pi^2)^2 - 4\omega_\pi^2 k_0^2}\right.\right. \\
&\qquad \left. - \frac{B_5 p^2}{(k_0^2 - m_\omega^2 + m_\pi^2)^2 - 4\omega_\pi^2 k_0^2}\right] \\
&\quad + \frac{n(\omega_a)}{\omega_a}\left[D_1 + \frac{D_2 + D_3 p^2}{(k_0^2 + m_{A_1}^2 - m_\pi^2)^2 - 4\omega_a^2 k_0^2}\right] \\
&\quad \left. - \frac{n(\omega_\omega)}{\omega_\omega}\left[\frac{D_4 p^2}{(k_0^2 + m_\omega^2 - m_\pi^2)^2 - 4\omega_\omega^2 k_0^2}\right]\right\},
\end{aligned}
\tag{34}
$$

where $p = |\mathbf{p}|$,

$$
\begin{aligned}
B_1 &= 4 - 16k_0^2\lambda_4 - 2\eta_2\bar{\eta}k_0^2, \\
B_2 &= \frac{4}{3}\left(4 + 4k_0^2\frac{\delta}{m_\rho^2} + k_0^4\frac{\delta^2}{m_\rho^4}\right), \\
B_3 &= 2k_0^2(k_0^2 - m_{A_1}^2 + m_\pi^2)\left[\bar{\eta}^2 m_\pi^2 + \eta_2^2(m_{A_1}^2 - m_\pi^2) + \eta_1\eta_2(k_0^2 - m_{A_1}^2 + m_\pi^2)\right], \\
B_4 &= 2k_0^2(k_0^2 - m_{A_1}^2 + m_\pi^2)\left[\bar{\eta}^2 - \frac{1}{3}\left(\bar{\eta}^2 - \frac{k_0^2\eta_1^2}{m_{A_1}^2}\right)\right], \\
B_5 &= \left(\frac{3g^2}{16\pi^4 F_\pi^2}\right)k_0^2(k_0^2 - m_\omega^2 + m_\pi^2)
\end{aligned}
\tag{35}
$$

and

$$
\begin{aligned}
D_1 &= 2k_0^2\eta_1\bar{\eta}, \\
D_2 &= 2k_0^2(k_0^2 + m_{A_1}^2 - m_\pi^2)\left[\bar{\eta}^2 m_{A_1}^2 - \eta_1^2(m_{A_1}^2 - m_\pi^2) + \eta_1\eta_2(k_0^2 + m_{A_1}^2 - m_\pi^2)\right], \\
D_3 &= 2k_0^2(k_0^2 + m_{A_1}^2 - m_\pi^2)\left[\bar{\eta}^2 - \frac{1}{3}\left(\bar{\eta}^2 - \frac{k_0^2\eta_1^2}{m_{A_1}^2}\right)\right], \\
D_4 &= \left(\frac{3g^2}{16\pi^4 F_\pi^2}\right)k_0^2(k_0^2 + m_\omega^2 - m_\pi^2).
\end{aligned}
\tag{36}
$$

The η_1, η_2, and λ_4 are given in Appendix B and $\bar{\eta} = (\eta_1 - \eta_2)^2$. We use the notation $\omega_\alpha = \sqrt{\mathbf{p}^2 + m_\alpha^2}$ ($\omega_a = \sqrt{p^2 + m_{A_1}^2}$) and $n(\omega_\alpha) = 1/(e^{\omega_\alpha/T} - 1)$.

There is only one diagram which contibutes to the self-energy of the ω meson at the one-loop level (Fig. 2). The explicit expression for this self-energy is given in Appendix C. We can see that the self-energy is transverse ($k^\mu\Pi_{\mu\nu}^\omega = 0$). We apply the following equation to determine the effective mass of the ω meson:

$$
k_0^2 - m_\omega^2 - F_\omega(k_0, \mathbf{k} \to 0) = 0, \tag{37}
$$

where

$$
\begin{aligned}
F_\omega(k_0, \mathbf{k} \to 0) &= G_\omega(k_0, \mathbf{k} \to 0) \\
&= -3g^2\int\frac{p^2dp}{(2\pi)^2}\left\{\frac{n(\omega_\rho)}{\omega_\rho}\left[\frac{C_1p^2}{(k_0^2 + m_\rho^2 - m_\pi^2)^2 - 4\omega_\rho^2k_0^2}\right] + \frac{n(\omega_\pi)}{\omega_\pi}\left[\frac{C_2p^2}{(k_0^2 - m_\rho^2 + m_\pi^2)^2 - 4\omega_\pi^2k_0^2}\right]\right\}
\end{aligned}
\tag{38}
$$

and

$$
\begin{aligned}
C_1 &= \left(\frac{3g^2}{16\pi^4 F_\pi^2}\right)k_0^2(k_0^2 + m_\rho^2 - m_\pi^2), \\
C_2 &= \left(\frac{3g^2}{16\pi^4 F_\pi^2}\right)k_0^2(k_0^2 - m_\rho^2 + m_\pi^2).
\end{aligned}
\tag{39}
$$

The A_1-meson self-energy is calculated from the diagrams in Fig. 3. Since the self-energy is not transverse and $k^\mu k^\nu\Pi_{\mu\nu}^{A_1} \neq 0$, there is no simple expression for the self-energy, and the general relation (27) should be used.

The expansion coefficients are related to the components of the self-energy as

$$
\begin{aligned}
\delta &= \frac{1}{k^2}k^\mu k^\nu\Pi_{\mu\nu}, \\
\gamma &= \frac{\sqrt{2}}{|\mathbf{k}|}(k^\mu\Pi_{\mu 0} - k_0\delta), \\
\beta &= \frac{1}{\mathbf{k}^2}(k^2\Pi_{00} - \sqrt{2}|\mathbf{k}|k_0\gamma - k_0^2\delta), \\
\alpha &= \tfrac{1}{2}(\Pi_\mu^\mu - \beta - \delta),
\end{aligned}
\tag{40}
$$

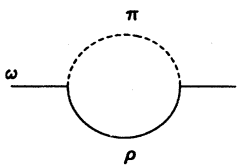

FIG. 2. One-loop contributions to the ω-meson self-energy.

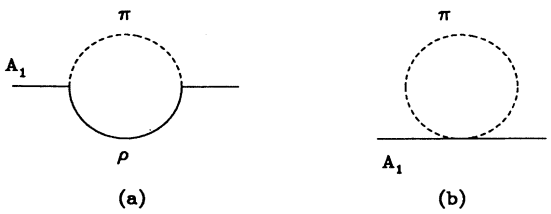

FIG. 3. One-loop contributions to the A_1-meson self-energy.

and the results are given in Appendix D. The δ and γ are not zero due to the nontransversality of the self-energy. The propagator can be obtained from Eq. (25):

$$\mathcal{D}^{\mu\nu} = \frac{1}{a}A^{\mu\nu} - \frac{2}{c^2+2bd}(dB^{\mu\nu} - cC^{\mu\nu} + bD^{\mu\nu}), \quad (41)$$

where the a, b, c, and d are related to the α, β, γ, and δ by

$$\begin{aligned} a &= k^2 - m_{A_1}^2 + \alpha, \\ b &= k^2 - m_{A_1}^2 + \beta, \\ c &= \gamma, \\ d &= -m_{A_1}^2 + \delta. \end{aligned} \quad (42)$$

The poles can be determined from the equations

$$a = k^2 - m_{A_1}^2 + \alpha = 0 \quad (43)$$

and

$$c^2 + 2bd = \gamma^2 - (\delta - m_{A_1}^2)(k^2 - m_{A_1}^2 + \beta) = 0. \quad (44)$$

The effective mass can be defined as the solutions of Eqs. (43) and (44) in the limit $\mathbf{k} \to 0$.

We find, in the limit $\mathbf{k} \to 0$, that

$$\begin{aligned} \delta(k_0, \mathbf{k}\to 0) &= -g^2 \int \frac{p^2 dp}{(2\pi)^2} \left\{ \frac{n(\omega_\pi)}{\omega_\pi} \left[\left(4\zeta_1 - \frac{\zeta_2}{2}p^2\right) - \frac{2\eta_1^2[(k_0^2+m_\pi^2)(k_0^2-m_\rho^2+m_\pi^2) - 4\omega_\pi^2 k_0^2]p^2}{(k_0^2-m_\rho^2+m_\pi^2)^2 - 4\omega_\pi^2 k_0^2} \right] \right. \\ &\quad \left. - \frac{n(\omega_\rho)}{\omega_\rho} \left[\frac{2\eta_1^2 m_\rho^2 (k_0^2+m_\rho^2-m_\pi^2)}{(k_0^2+m_\rho^2-m_\pi^2)^2 - 4\omega_\rho^2 k_0^2} \right] \right\}, \\ \gamma(k_0, \mathbf{k}\to 0) &\to 0, \\ \alpha(k_0, \mathbf{k}\to 0) &= \beta(k_0, \mathbf{k}\to 0), \end{aligned} \quad (45)$$

where the ζ's are given in Appendix D. Thus the effective mass of the A_1 meson can be determined from the single equation

$$k_0^2 - m_{A_1}^2 + \alpha(k_0, \mathbf{k}\to 0) = 0. \quad (46)$$

Here

$$\begin{aligned} \alpha(k_0, \mathbf{k}\to 0) &= \beta(k_0, \mathbf{k}\to 0) \\ &= -g^2 \int \frac{p^2 dp}{(2\pi)^2} \left\{ \frac{n(\omega_\pi)}{\omega_\pi} \left[C - \frac{4}{3}\zeta_2 p^2 + \frac{F_1 + F_2 p^2 - F_3 p^4}{(k_0^2-m_\rho^2+m_\pi^2)^2 - 4\omega_\pi^2 k_0^2} \right] \right. \\ &\quad \left. + \frac{n(\omega_\rho)}{\omega_\rho} \left[\frac{G_1 + G_2 p^2}{(k_0^2+m_\rho^2-m_\pi^2)^2 - 4\omega_\rho^2 k_0^2} \right] \right\}, \end{aligned} \quad (47)$$

where

$$\begin{aligned} C &= -4(\zeta_1 + m_\pi^2\zeta_2 + k_0^2\zeta_3), \\ F_1 &= 2(k_0^2 - m_\rho^2 + m_\pi^2)[(k_0^2+m_\pi)(\eta_1^2 m_\pi^2 + \eta_2^2 k_0^2) + 4\eta_1\eta_2 k_0^2 m_\pi^2] - 8k_0^2 m_\pi^2[\eta_1^2 m_\pi^2 + \eta_2^2 k_0^2 + \eta_1\eta_2(k_0^2+m_\pi^2)], \\ F_2 &= \tfrac{2}{3}(k_0^2 - m_\rho^2 + m_\pi^2)[\eta_1^2(k_0^2+m_\pi^2) + 2k_0^2(\eta_1^2+\eta_2^2+4\eta_1\eta_2)] - \tfrac{8}{3}k_0^2[4\eta_1^2 m_\pi^2 + 3\eta_2^2 k_0^2 + 3\eta_1\eta_2(k_0^2+m_\pi^2)], \\ F_3 &= \tfrac{8}{3}\eta_1^2 k_0^2 \end{aligned} \quad (48)$$

and

$$\begin{aligned} G_1 &= 2(k_0^2 + m_\rho^2 - m_\pi^2)m_\rho^2(\eta_1^2 m_\rho^2 + k_0^2\bar{\eta}^2) - 8k_0^2 m_\rho^4 \eta_1\bar{\eta}, \\ G_2 &= \tfrac{2}{3}(k_0^2 + m_\rho^2 - m_\pi^2)(\eta_1^2 m_\rho^2 + 2k_0^2\bar{\eta}^2) - 8k_0^2 m_\rho^2 \eta_1\bar{\eta}. \end{aligned} \quad (49)$$

The equations for effective masses [Eqs. (33), (37), and (46)] can be solved self-consistently. The results are shown in Fig. 4. Even though the numerical values are different for the two parameter sets, the ρ-meson mass increases and the A_1-meson mass decreases with temperature in both cases. The A_1-meson mass is changed very slowly when $T < 200$ MeV, but the ρ-meson mass increases contantly from $T \approx 50$ MeV for parameter set I. For parameter set II the A_1-meson mass decreases rather rapidly with temperature, but the ρ-meson mass is almost constant. The ρ-meson and A_1-meson masses are equal at $T \approx 220$ MeV for both parameter sets.

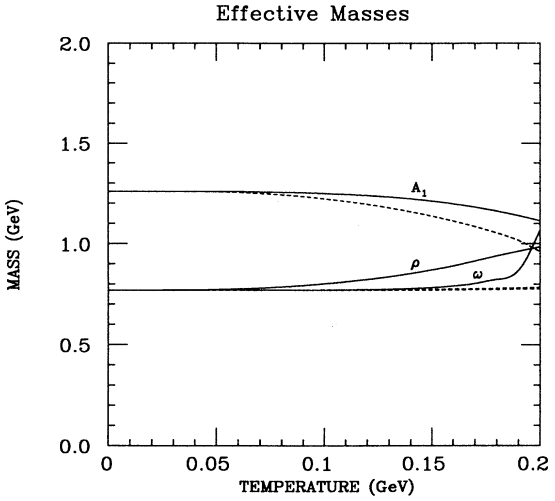

FIG. 4. Effective masses determined from the pole positions of the propagators for parameter set I (solid line) and set II (dashed line). For parameter set II the ρ-meson and ω-meson masses are almost constant at all temperatures.

For the ω meson, temperature effects are small for both parameter sets. As the temperature increases the ρ-meson and ω-meson masses split. For parameter set I the splitting is rather obvious, but for parameter set II the difference is small (about 10 MeV at $T = 200$ MeV).

IV. SCREENING MASS

Lattice calculations are performed in Euclidean space, or imaginary time. To determine the pole of a propagator in Minkowski space, or real time, an analytic continuation must be done. So far, lattices used in Monte Carlo calculations are too small to carry out a meaningful analytic continuation. Instead, the correlator of static operators is considered:

$$S_{AB}(z) = \langle \bar{A}(z)\bar{B}(0)\rangle - \langle \bar{A}(0)\rangle\langle \bar{B}(0)\rangle, \tag{50}$$

where A and B are local operators and the averages, represented by angular brackets are taken over the Gibbs ensemble at temperature T [6]. The large-distance behavior of this correlator defines a screening mass $\mu(T)$:

$$S_{AB}(z) \longrightarrow b\exp[-\mu(T)|z|] \quad \text{as} \quad |z| \to \infty. \tag{51}$$

It is expected that the low-lying excitation of the plasma may be related to the screening effects just as the plasmon in an ordinary electromagnetic plasma is associated with the phenomenon of Debye screening.

In finite-temperature field theory, the static-screening mass can be obtained from linear-response analysis [1,32,33]. When we apply an external, static electric field $E_{\rm cl}$ to the QED plasma, the net electric field in the medium is

$$E_i^{\rm net}(\mathbf{x}) = -\int \frac{d^3k}{(2\pi)^3}\, e^{i\mathbf{k}\cdot\mathbf{x}} E_j^{\rm cl}(\mathbf{k}) \times\{k_ik_jD_{00}^R(\omega,\mathbf{k}) + \omega k_iD_{0j}^R(\omega,\mathbf{k}) + \omega k_jD_{i0}^R(\omega,\mathbf{k}) + \omega^2 D_{ij}^R(\omega,\mathbf{k})\}_{\omega=0}, \tag{52}$$

where $D_{\mu\nu}^R$ is the retarded Green's function and related to the imaginary-time propagator ($\mathcal{D}_{\mu\nu}$) by analytic continuation:

$$D_{\mu\nu}^R(\omega,\mathbf{k}) = \mathcal{D}_{\mu\nu}(i\omega_n \to \omega + i\epsilon, \mathbf{k}), \quad \epsilon \to 0^+. \tag{53}$$

In the covariant gauge, the photon propagator is given by

$$\mathcal{D}^{\mu\nu} = \frac{1}{G_\gamma - k^2}P_T^{\mu\nu} + \frac{1}{F_\gamma - k^2}P_L^{\mu\nu} + \frac{\rho}{k^2}\frac{k^\mu k^\nu}{k^2} \tag{54}$$

and the net electric field in momentum space is

$$E_i^{\rm net} = \frac{k_ik_jE^{j\rm cl}(\mathbf{k})}{\mathbf{k}^2 + F_\gamma(\omega = 0,\ \mathbf{k})}. \tag{55}$$

The potential between two static charges (Q_1 at $\mathbf{x}_1$ and Q_2 at $\mathbf{x}_2$) then can be written

$$V(\mathbf{R} = \mathbf{x}_1 - \mathbf{x}_2) = Q_1Q_2\int \frac{d^3k}{(2\pi)^3}e^{i\mathbf{k}\cdot\mathbf{R}}\frac{1}{\mathbf{k}^2 + F_\gamma(0,\mathbf{k})}. \tag{56}$$

For large R, we obtain a screened Coulomb potential with inverse screening length $m_{\rm el}$:

$$V(R) \approx \frac{Q_1Q_2}{4\pi}\frac{e^{-m_{\rm el}R}}{R}, \tag{57}$$

where $R = |\mathbf{R}|$ and

$$m_{\rm el}^2 = F_\gamma\ (\omega = 0, \mathbf{k} \to 0). \tag{58}$$

For the ρ meson the propagator is given by Eq. (32). The last three terms vanish in Eq. (52). Thus the net "electric" field is

$$E_i^{\rm net} = \frac{k_ik_jE^{j\rm cl}(\mathbf{k})}{\mathbf{k}^2 + F_\rho(\omega = 0,\ \mathbf{k}) + m_\rho^2}. \tag{59}$$

The screening mass can be obtained from the F by

$$m_\rho^{\rm sc} = \sqrt{m_\rho^2 + F_\rho(\omega = 0,\ \mathbf{k} \to 0)}. \tag{60}$$

F is related to the time-time component of the self-energy, and in the limit $\omega = 0$ and $\mathbf{k} \to 0$ it can be written as

$$F_\rho(\omega = 0, \mathbf{k} \to 0) = -\Pi_\rho^{00}. \tag{61}$$

We find that

$$F_\rho(\omega = 0, \mathbf{k} \to 0) = 4g^2\int \frac{dp}{(2\pi)^2}\frac{n(\omega_\pi)}{\omega_\pi}\left(m_\pi^2 + 2p^2\right). \tag{62}$$

There are no contributions from the diagrams which include more than one species of hadrons. For example, there are none from the A_1-π loop [Fig. 1(c)] or from the ω-π loop [Fig. 1(d)].

We can apply the same relations for the ω-meson screening mass as for the ρ-meson screening mass. We find that the time-time component of the ω-meson self-energy vanishes in the limit considered:

$$\Pi_\omega^{00}(\omega = 0, \mathbf{k} \to 0) = 0. \tag{63}$$

This is consistent with the rules mentioned above since there is only a diagram which includes the ρ meson and pion in the loop. We have

$$m_\omega^{sc} = m_\omega. \tag{64}$$

Thus the screening mass of the ω meson has no temperature dependence.

Because of the nontransversality of the A_1-meson self-energy, we have a complicated relation for net "electric" fields:

$$E_i^{\text{net}} = \frac{-2(m_{A_1}^2 - \delta)}{2(\mathbf{k}^2 - m_{A_1}^2 + \beta)(m_{A_1}^2 - \delta) + \gamma^2} k_i k_j E^{j\text{cl}}(\mathbf{k}). \tag{65}$$

But in the limit considered,

$$\beta = -g^2 \int \frac{dp}{(2\pi)^2} \left\{ \frac{n(\omega_\pi)}{\omega_\pi} \left[\eta_1^2 \frac{2m_\pi^2 p^4}{m_\rho^2 - m_\pi^2} - 4(\zeta_1 p^2 - \zeta_2 p^4) \right] - \frac{n(\omega_\rho)}{\omega_\rho} \eta_1^2 \frac{2m_\rho^2 p^4}{m_\rho^2 - m_\pi^2} \right\}, \tag{66}$$

$$\gamma \to 0, \tag{67}$$

$$\delta = -g^2 \int \frac{dp}{(2\pi)^2} \left\{ \frac{n(\omega_\pi)}{\omega_\pi} \left[\left(\zeta_1 + \zeta_2 m_\pi^2 + \frac{2\eta_1^2 m_\pi^4}{m_\rho^2 - m_\pi^2} \right) p^2 + \frac{1}{3}(\zeta_2 + 2\eta_1^2) p^4 \right] + \frac{n(\omega_\rho)}{\omega_\rho} \frac{2\eta_1^2 m_\rho^4}{m_\rho^2 - m_\pi^2} p^2 \right\}, \tag{68}$$

and so we have

$$m_{A_1}^{sc} = \sqrt{m_{A_1}^2 - \beta(0, \mathbf{k} \to 0)}. \tag{69}$$

The results of our one-loop computations of the screening masses of the ρ meson, ω meson, and A_1 meson are shown in Fig. 5. We get the same behavior with temperature as the effective masses determined from the pole positions of the propagator. But the numerical values are quite different. The ρ-meson mass becomes equal to the A_1-meson mass at $T \approx 160$ MeV for parameter set I and at $T \approx 240$ MeV for parameter set II. The mass splitting of the ρ and ω mesons are rather obvious.

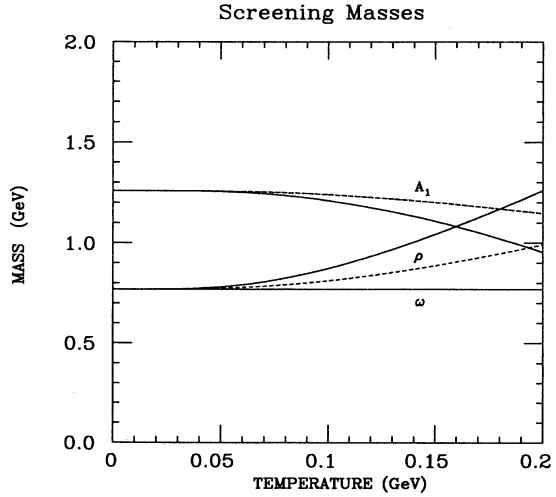

FIG. 5. Screening masses of the vector and axial-vector mesons for parameter set I (solid line) and set II (dashed line). For the ω meson the screening mass does not change with temperature.

We can also obtain the physical electric screening mass of the hadronic system, which is defined as the inverse Debye screening length. It is related to the photon self-energy by

$$m_{\text{el}}^2 = -\Pi_\gamma^{00}(\omega = 0, \mathbf{k} \to 0). \tag{70}$$

The photon self-energy at the lowest order can be directly related to the neutral ρ-meson self-energy and the ω-meson self-energy:

$$\Pi_\gamma^{\mu\nu} = \frac{2e^2}{g^2} \left(\Pi_\rho^{\mu\nu} + \Pi_\omega^{\mu\nu} \right). \tag{71}$$

The electric screening mass can be obtained from Eqs. (62) and (63):

$$m_{\text{el}}^2 = \frac{2}{\pi^2} \int dp \frac{n(\omega_\pi)}{\omega_\pi} (m_\pi^2 + 2p^2), \tag{72}$$

which is exactly the same result as that in Ref. [34]. Note that there are no contributions from the loop diagrams which include two different mesons as mentioned in Sec. III [Figs. 1(c), 1(d), and 2]. This is consistent with the theorem discussed in Ref. [34].

V. CONCLUSION

We have described hadronic matter by an effective chiral Lagrangian with pions, ρ mesons, ω mesons, and A_1 mesons. It is possible to obtain some information about hot hadronic matter from the effective masses of the

mesons at finite temperature. We calculated the masses of the mesons at finite temperature in two different ways: the pole mass computed from the pole positions of the propagator (Sec. III) and the screening mass determined by the large-distance behavior of the hadronic correlation function (Sec. IV).

Even though the numerical values depend on the parameters used, we found that the effective mass of the ρ meson increases with temperature. This result is consistent with that of Gale and Kapusta who used an effective Lagrangian with charged pions and neutral ρ mesons only [10]. Inclusion of the A_1 meson in the system changes the numerical results but not the behavior with temperature of the effective ρ-meson mass. For the screening mass there are no contributions from the diagrams which include the A_1 mesons. On the other hand, the A_1-meson mass decreases and the ρ- and A_1-meson masses get closer as temperature increases. The effective mass of the ω meson is not changed too much with temperature, although the difference between the ρ- and ω-meson masses becomes bigger as temperature increases.

The screening masses of the mesons show a behavior with temperature similar to that of the pole masses, but the numerical values are different. The screening masses are not identical with the effective masses determined from the pole positions of the propagators. However, the qualitative properties at finite temperature are the same. From these results we infer the following conclusions.

A. Chiral-symmetry restoration

It is believed that the order parameter of the chiral-symmetry breaking and restoration is the quark condensate $\langle\bar{q}q\rangle$. Chiral-symmetry restoration at high temperature has been inferred from the decrease of the condensate as temperature increases [35]. Since the condensate is not directly related to measureable quantities, we consider instead the consequences of the restoration of the symmetry in the hadron spectrum. It is expected that pions, which are Goldstone bosons, get mass after symmetry restoration, and there may be chiral multiplets in the hadron spectrum.

It has been suggested that the degeneracies of the hadronic screening masses in the expected chiral multiplets indicate chiral-symmetry restoration [6]. Even though the screening mass is not necessarily the same as the real excitations in hot hadronic matter, it has information about the symmetry properties of the hadronic matter. Lattice simulations have shown that there are degeneracies at high temperature, and the conclusions are consistent with the results obtained from the calculation of the quark condensate [6,7].

We calculated the screening masses of the ρ and A_1 mesons at low temperatures ($T < T_{\rm ch}$) and found that the ρ-meson and the A_1-meson screening masses get close as the temperature increases. This is consistent with the lattice calculations which show the mass degeneracies above $T_{\rm ch}$ and suggest chiral-symmetry restoration. The results obtained here suggest chiral-symmetry restoration, but do not prove it.

As temperature increases, a deconfinement phase transition is expected. The phase transition might occur about $T_d = 150$–200 MeV. This phase transition is crucial in our conclusion because obviously the effective Lagrangian cannot be applied after the transition. There are also some effects coming from the heavier mesons which are not included in the present model. Thus we view our results as reliable up to about $T = 150$ MeV.

The nonlinear σ model is based on the spontaneous breaking of the chiral symmetry and cannot be applied after the restoration of the symmetry. The results have some ambiguities near the phase transiton in this sense. If we regard the degeneracy of the screening masses as the signal of the symmetry restoration, the results after the degeneracy point do not mean anything.

B. Zweig rule

The ω-meson mass is not changed too much by temperature. Even if we start with the same mass for the ρ meson and ω meson at zero temperature, these masses are split at finite temperature. Such a splitting of the mass at finite temperature was also reported in Ref. [9], which used QCD sum rules. The ρ-meson and ω-meson masses can be written as the expectation values of the Hamiltonian [36]:

$$m_\rho \sim \langle d\bar{d} - u\bar{u}|H|d\bar{d} - u\bar{u}\rangle, \tag{73}$$

$$m_\omega \sim \langle d\bar{d} + u\bar{u}|H|d\bar{d} + u\bar{u}\rangle. \tag{74}$$

The mass differences between these mesons are related to the flavor-changing processes:

$$m_\rho - m_\omega \sim \langle d\bar{d}|H|u\bar{u}\rangle. \tag{75}$$

Thus the Zweig rule, which forbids flavor-changing transitions, might not work anymore at finite temperature.

C. Dilepton emission in the medium

The dilepton emission rates from the hadronic processes are interesting because they may probe the properties of hot matter, as studied here. The emission rates depend on the properties of the mesons, the mass, and the decay width. Since pion annihilation through the ρ meson is the dominant channel in the production of the dileptons in hadronic matter, the changes of the ρ-meson properties in the medium will affect the emission rates. Increase of the ρ-meson mass is expected to shift the ρ-meson peak in the dilepton mass spectrum [10]. The details will appear elsewhere.

ACKNOWLEDGMENTS

I am very grateful to J. I. Kapusta for many useful discussions and a critical reading of the manuscript. I also thank V. Eletsky for helpful conversations. This research

was supported by the U.S. Department of Energy under Grant No. DOE/DE-FG02-87ER-40328.

APPENDIX A: DEFINITIONS OF FUNCTIONS

The angle integration in the self-energy can be expressed in terms of the integrals

$$
\begin{aligned}
A_n &= \int_{-1}^{1} dy \frac{(pky)^n}{(k_0^2 - k^2 + m^2) + 2\omega k_0 + 2pky}, \\
B_n &= \int_{-1}^{1} dy \frac{(pky)^n}{(k_0^2 - k^2 + m^2) - 2\omega k_0 + 2pky}, \\
C_n &= \int_{-1}^{1} dy \frac{(pky)^n}{(k_0^2 - k^2 + m^2) + 2\omega k_0 - 2pky} \\
&= (-1)^n A_n, \\
D_n &= \int_{-1}^{1} dy \frac{(pky)^n}{(k_0^2 - k^2 + m^2) - 2\omega k_0 - 2pky} \\
&= (-1)^n B_n,
\end{aligned}
\tag{A1}
$$

where $p = |\mathbf{p}|$ and $k = |\mathbf{k}|$. For convenience define

$$
\begin{aligned}
\Lambda_n^+ &= A_n + B_n, \\
\Lambda_n^- &= A_n - B_n.
\end{aligned}
\tag{A2}
$$

The one-dimensional integration can be easily done, and the results are

$$
\begin{aligned}
\Lambda_0^+ &= \frac{1}{2pk} L^+, \\
\Lambda_0^- &= \frac{1}{2pk} L^-, \\
\Lambda_1^+ &= 2 - \frac{k_0^2 - k^2 + m^2}{4pk} L^+ - \frac{k_0\omega}{2pk} L^-, \\
\Lambda_1^- &= -\frac{k_0\omega}{2pk} L^+ - \frac{k_0^2 - k^2 + m^2}{4pk} L^-,
\end{aligned}
\tag{A3}
$$

$$
\begin{aligned}
\Lambda_2^+ &= -(k_0^2 - k^2 + m^2) + \frac{(k_0^2 - k^2 + m^2)^2 + 4\omega^2 k_0^2}{8pk} L^+ \\
&\quad + \frac{k_0\omega(k_0^2 - k^2 + m^2)}{2pk} L^-, \\
\Lambda_2^- &= -2k_0\omega - \frac{k_0\omega(k_0^2 - k^2 + m^2)}{2pk} L^+ \\
&\quad - \frac{(k_0^2 - k^2 + m^2)^2 + 4\omega^2 k_0^2}{8pk} L^-, \\
\Lambda_3^+ &= \frac{2}{3} p^2 k^2 + \frac{1}{2} \left[(k_0^2 - k^2 + m^2)^2 + 4\omega^2 k_0^2 \right] \\
&\quad - \frac{(k_0^2 - k^2 + m^2)^3 + 12 k_0^2 \omega^2 (k_0^2 - k^2 + m^2)}{16pk} L^+ \\
&\quad - \frac{6k_0\omega(k_0^2 - k^2 + m^2)^2 + 8k_0^3\omega^3}{16pk} L^-,
\end{aligned}
$$

where

$$
\begin{aligned}
L^+ &= \ln \frac{(k_0^2 - k^2 + m^2 + 2pk)^2 - 4\omega^2 k_0^2}{(k_0^2 - k^2 + m^2 - 2pk)^2 - 4\omega^2 k_0^2}, \\
L^- &= \ln \frac{(k_0^2 - k^2 + m^2)^2 - 4(\omega k_0 + pk)^2}{(k_0^2 - k^2 + m^2)^2 - 4(\omega k_0 - pk)^2}.
\end{aligned}
\tag{A4}
$$

APPENDIX B: ρ-MESON SELF-ENERGY

There are four diagrams which contribute to the ρ-meson self-energy (see Fig. 1):

$$
\Pi_{\mu\nu}^{\rho} = \Pi_{\mu\nu}^{\rho(a)} + \Pi_{\mu\nu}^{\rho(b)} + \Pi_{\mu\nu}^{\rho(c)} + \Pi_{\mu\nu}^{\rho(d)}. \tag{B1}
$$

(1) The contributions from the pion loops, $\Pi_{\mu\nu}^{\rho\,(\mathrm{I})}$:

$$
\Pi_{\mu\nu}^{\rho\,(\mathrm{I})} = \Pi_{\mu\nu}^{\rho\,(a)} + \Pi_{\mu\nu}^{\rho\,(b)}, \tag{B2}
$$

$$
\Pi_{00}^{\rho\,(\mathrm{I})} = 4g^2 \int \frac{p^2 dp}{(2\pi)^2} \frac{n(\omega_\pi)}{\omega_\pi} \left[(D_1 + \lambda_4 k^2) - D_2 \left(\frac{k_0^2 + 4\omega_\pi^2}{8pk} \right) L_0^+ - D_2 \left(\frac{k_0\omega_\pi}{2pk} \right) L_0^- \right], \tag{B3}
$$

$$
\Pi_{\mu}^{\mu\rho\,(\mathrm{I})} = 4g^2 \int \frac{p^2 dp}{(2\pi)^2} \frac{n(\omega_\pi)}{\omega_\pi} \left[(3 - D_1 + 3\lambda_4 k^2) - D_2 \left(\frac{k_0^2 - k^2 + 4m_\pi^2}{8pk} \right) L_0^+ \right], \tag{B4}
$$

where

$$
\begin{aligned}
&p=|\mathbf{p}| \quad \text{and} \quad k=|\mathbf{k}|, \\
&\delta=1-\frac{(1-\sigma)m_\rho^2}{(1+\sigma)m_{A_1}^2}-\frac{2\xi g}{\sqrt{1-\sigma}}\left(\frac{1-\sigma}{1+\sigma}\right)\frac{m_\rho^4}{m_{A_1}^4}\left(1-\frac{(1-\sigma)m_\rho^2}{(1+\sigma)m_{A_1}^2}\right)^{-1}, \\
&\lambda_4=\left(\frac{1-\sigma}{1+\sigma}\right)\frac{g^2F_\pi^2}{16m_\rho^4}-\frac{\sigma}{m_\rho^2(1-\sigma)}+\frac{2}{g^2F_\pi^2}\frac{\sigma^2}{1-\sigma},
\end{aligned}
\tag{B5}
$$

$$
\begin{aligned}
&D_1=1+k_0^2\frac{\delta}{m_\rho^2}+k_0^2(k_0^2-k^2)\frac{\delta^2}{4m_\rho^4}, \\
&D_2=1+(k_0^2-k^2)\frac{\delta}{m_\rho^2}+(k_0^2-k^2)^2\frac{\delta^2}{4m_\rho^4}, \\
&L_0^\pm=L^\pm(\omega=\omega_\pi,\ m^2=0).
\end{aligned}
$$

(2) The contributions from the A_1-meson loops , $\Pi_{\mu\nu}^{\rho\,(\mathrm{II})}$:

$$
\Pi_{\mu\nu}^{\rho\,(\mathrm{II})}=\Pi_{\mu\nu}^{\rho\,(c)}, \tag{B6}
$$

$$
\begin{aligned}
\Pi_{00}^{\rho\,(\mathrm{II})}=g^2\int\frac{p^2dp}{(2\pi)^2}\Bigg\{&\frac{n(\omega_\pi)}{\omega_\pi}\Bigg[-\frac{1}{2}H_1(k_0^2-k^2-m_{A_1}^2+m_\pi^2)-2(\eta_2^2-\eta_1\eta_2)k^2 \\
&+\frac{1}{16pk}[H_1(k_0^2-k^2-m_{A_1}^2+m_\pi^2)^2 \\
&+4H_2\omega_\pi^2(k_0^2-k^2)-4H_3k^2]L_\pi^+ +\frac{H_2k_0\omega_\pi(k_0^2-k^2-m_{A_1}^2+m_\pi^2)}{4pk}L_\pi^-\Bigg] \\
&+\frac{n(\omega_a)}{\omega_a}\Bigg[-\frac{1}{2}H_1(k_0^2-k^2+m_{A_1}^2-m_\pi^2)-2(\eta_1^2-\eta_1\eta_2)k^2 \\
&+\frac{1}{16pk}[H_1(k_0^2-k^2+m_{A_1}^2-m_\pi^2)^2+4H_2\omega_a^2(k_0^2-k^2)-4H_3k^2]L_a^+ \\
&+\frac{H_2k_0\omega_a(k_0^2-k^2+m_{A_1}^2-m_\pi^2)}{4pk}L_a^-\Bigg]\Bigg\},
\end{aligned}
\tag{B7}
$$

$$
\begin{aligned}
\Pi_{\mu}^{\mu\rho\,(\mathrm{II})}=g^2\int\frac{p^2dp}{(2\pi)^2}\Bigg\{&\frac{n(\omega_\pi)}{\omega_\pi}\Bigg[-\frac{1}{2}\bar{H}_2(k_0^2-k^2-m_{A_1}^2+m_\pi^2)+6(\eta_2^2-\eta_1\eta_2)(k_0^2-k^2) \\
&+\frac{1}{16pk}[\bar{H}_2(k_0^2-k^2-m_{A_1}^2+m_\pi^2)^2+(4H_2m_\pi^2+3H_3)(k_0^2-k^2)]L_\pi^+\Bigg] \\
&+\frac{n(\omega_a)}{\omega_a}\Bigg[-\frac{1}{2}\bar{H}_2(k_0^2-k^2+m_{A_1}^2-m_\pi^2)+6(\eta_1^2-\eta_1\eta_2)(k_0^2-k^2) \\
&+\frac{1}{16pk}[\bar{H}_2(k_0^2-k^2+m_{A_1}^2-m_\pi^2)^2+(4H_2m_a^2-3H_4)(k_0^2-k^2)]L_a^+\Bigg]\Bigg\},
\end{aligned}
\tag{B8}
$$

where

$$\eta_1 = \frac{2}{gF_\pi}\left(\frac{1-\sigma}{1+\sigma}\right)^{\frac{1}{2}}\left(1-\frac{(1-\sigma)m_\rho^2}{(1+\sigma)m_{A_1}^2}\right)+\frac{4\xi}{F_\pi\sqrt{1+\sigma}}\frac{(1-\sigma)m_\rho^2}{(1+\sigma)m_{A_1}^2},$$
$$\eta_2 = \frac{2}{gF_\pi}\left(\frac{1+\sigma}{1-\sigma}\right)^{\frac{1}{2}}\left(1-\frac{(1-\sigma)m_\rho^2}{(1+\sigma)m_{A_1}^2}\right)-\frac{4\sigma}{gF_\pi\sqrt{1-\sigma^2}},$$
$$H_1 = (\eta_1-\eta_2)^2-\frac{\eta_1^2k_0^2}{m_{A_1}^2},$$
$$H_2 = (\eta_1-\eta_2)^2-\frac{\eta_1^2(k_0^2-k^2)}{m_{A_1}^2},$$
$$\bar{H}_2 = 3(\eta_1-\eta_2)^2-H_2, \tag{B9}$$
$$H_3 = \eta_2^2(m_{A_1}^2-m_\pi^2)+\eta_1\eta_2(k_0^2-k^2-m_{A_1}^2+m_\pi^2),$$
$$H_4 = \eta_1^2(m_{A_1}^2-m_\pi^2)-\eta_1\eta_2(k_0^2-k^2+m_{A_1}^2-m_\pi^2),$$
$$L_\pi^\pm = L^\pm(\omega=\omega_\pi,\ m^2=m_\pi^2-m_{A_1}^2),$$
$$L_a^\pm = L^\pm(\omega=\omega_a,\ m^2=m_{A_1}^2-m_\pi^2).$$

(3) The contributions from the ω-meson loops, $\Pi_{\mu\nu}^{\rho\,(\mathrm{III})}$:

$$\Pi_{\mu\nu}^{\rho\,(\mathrm{III})} = \Pi_{\mu\nu}^{\rho\,(d)}, \tag{B10}$$

$$\Pi_{00}^{\rho\,(\mathrm{III})} = \frac{1}{2}g_\omega^2\int\frac{p^2dp}{(2\pi)^2}\left\{\frac{n(\omega_\pi)}{\omega_\pi}\left[(k_0^2-k^2-m_\omega^2+m_\pi^2)^2\right.\right.$$
$$\left.-\frac{(k_0^2-k^2-m_\omega^2+m_\pi^2)^2+4\omega_\pi^2k_0^2-4p^2k^2}{8pk}\tilde{L}_\pi^+\right.$$
$$\left.-\frac{k_0\omega_\pi(k_0^2-k^2-m_\omega^2+m_\pi^2)}{2pk}\tilde{L}_\pi^-\right]$$
$$+\frac{n(\omega_\omega)}{\omega_\omega}\left[(k_0^2-k^2+m_\omega^2-m_\pi^2)^2-\frac{(k_0^2-k^2+m_\omega^2-m_\pi^2)^2+4\omega_\omega^2k_0^2-4p^2k^2}{8pk}L_\omega^+\right.$$
$$\left.\left.-\frac{k_0\omega_\omega(k_0^2-k^2+m_\omega^2-m_\pi^2)}{2pk}L_\omega^-\right]\right\}, \tag{B11}$$

$$\Pi_\mu^{\mu\rho\,(\mathrm{III})} = g_\omega^2\int\frac{p^2dp}{(2\pi)^2}\left\{\frac{n(\omega_\pi)}{\omega_\pi}\left[(k_0^2-k^2-m_\omega^2+m_\pi^2)^2-\frac{(k_0^2-k^2-m_\omega^2+m_\pi^2)^2-4m_\pi^2(k_0^2-k^2)}{8pk}\tilde{L}_\pi^+\right]\right.$$
$$+\frac{n(\omega_\omega)}{\omega_\omega}\left[(k_0^2-k^2+m_\omega^2-m_\pi^2)^2\right.$$
$$\left.\left.-\frac{(k_0^2-k^2+m_\omega^2-m_\pi^2)^2-4m_\pi^2(k_0^2-k^2)}{8pk}L_\omega^+\right]\right\}, \tag{B12}$$

where

$$g_\omega = \left(\frac{3g^2}{8\pi^2F_\pi}\right),$$
$$\tilde{L}_\pi^\pm = L^\pm(\omega=\omega_\pi,\ m^2=m_\pi^2-m_\omega^2),$$
$$L_\omega^\pm = L^\pm(\omega=\omega_\omega,\ m^2=m_\omega^2-m_\pi^2). \tag{B13}$$

APPENDIX C: ω-MESON SELF-ENERGY

There is only one diagram for the ω self-energy (Fig. 2). The Π^{ω}_{00} and $\Pi^{\mu\omega}_{\mu}$ are given by

$$\Pi^{\omega}_{00} = \frac{3}{2}g^2_{\omega}\int\frac{p^2dp}{(2\pi)^2}\left\{\frac{n(\omega_\pi)}{\omega_\pi}\left[(k_0^2-k^2-m_\rho^2+m_\pi^2)^2-\frac{(k_0^2-k^2-m_\rho^2+m_\pi^2)^2+4\omega_\pi^2k_0^2-4p^2k^2}{8pk}L^+_\pi\right.\right.$$
$$\left.-\frac{k_0\omega_\pi(k_0^2-k^2-m_\rho^2+m_\pi^2)}{2pk}L^-_\pi\right]$$
$$+\frac{n(\omega_\rho)}{\omega_\rho}\left[(k_0^2-k^2+m_\rho^2-m_\pi^2)^2\right.$$
$$-\frac{(k_0^2-k^2+m_\rho^2-m_\pi^2)^2+4\omega_\rho^2k_0^2-4p^2k^2}{8pk}L^+_\rho$$
$$\left.\left.-\frac{k_0\omega_\rho(k_0^2-k^2+m_\rho^2-m_\pi^2)}{2pk}L^-_\rho\right]\right\}, \tag{C1}$$

$$\Pi^{\mu\omega}_{\mu} = 3g^2_{\omega}\int\frac{p^2dp}{(2\pi)^2}\left\{\frac{n(\omega_\pi)}{\omega_\pi}\left[(k_0^2-k^2-m_\rho^2+m_\pi^2)^2-\frac{(k_0^2-k^2-m_\rho^2+m_\pi^2)^2-4m_\pi^2(k_0^2-k^2)}{8pk}L^+_\pi\right]\right.$$
$$\left.+\frac{n(\omega_\rho)}{\omega_\rho}\left[(k_0^2-k^2+m_\rho^2-m_\pi^2)^2-\frac{(k_0^2-k^2+m_\rho^2-m_\pi^2)^2-4m_\pi^2(k_0^2-k^2)}{8pk}L^+_\rho\right]\right\}, \tag{C2}$$

where

$$L^{\pm}_\pi = L^{\pm}(\omega=\omega_\pi,\ m^2=m_\pi^2-m_\rho^2),$$
$$L^{\pm}_\rho = L^{\pm}(\omega=\omega_\rho,\ m^2=m_\rho^2-m_\pi^2). \tag{C3}$$

APPENDIX D: A_1-MESON SELF-ENERGY

We consider two diagrams (Fig. 3) and obtain the self-energy

$$k^\mu k^\nu\Pi^{A_1}_{\mu\nu} = -g^2\int\frac{p^2dp}{(2\pi)^2}\left\{\frac{n(\omega_\pi)}{\omega_\pi}\eta_1^2\left[\frac{\omega_\pi k_0[m_\pi^2(k_0^2-k^2)-\omega_\pi^2k_0^2]}{2pk}L^-_\pi-\frac{(p^2k_0^2+m_\pi^2k^2)(k_0^2-k^2+m_\pi^2)}{4pk}L^+_\pi\right.\right.$$
$$+[m_\pi^2(k_0^2-k^2)-3\omega_\pi^2k_0^2]\Lambda^+_{p1}-\omega_\pi k_0(k_0^2-k^2+m_\pi^2)\Lambda^-_{p1}$$
$$\left.-\frac{1}{2}(k_0^2-k^2+m_\pi^2)\Lambda^+_{p2}-3\omega_\pi k_0\Lambda^-_{p2}-\Lambda^+_{p3}\right]$$
$$-\frac{n(\omega_\rho)}{\omega_\rho}\eta_1^2\left[\frac{m_\rho^2(p^2k_0^2-m_\rho^2k^2)}{4pk}L^+_\rho+\omega_\rho k_0m_\rho^2\Lambda^-_{r1}+\frac{1}{2}m_\rho^2\Lambda^+_{r2}\right]$$
$$\left.-\frac{n(\omega_\pi)}{\omega_\pi}4\left[\zeta_1(k_0^2-k^2)-\zeta_2[m_\pi^2k^2-k_0^2p^2-\tfrac{1}{3}k^2p^2]\right]\right\}, \tag{D1}$$

$$k^\mu k^0\Pi^{A_1}_{\mu0} = g^2\int\frac{p^2dp}{(2\pi)^2}\left\{\frac{n(\omega_\pi)}{\omega_\pi}\left[4(\zeta_1-\zeta_2p^2)k_0^2+\frac{\eta_1^2p^2k_0^2(k_0^2-k^2+m_\pi^2)-2\eta_1\eta_2\omega_\pi^2k^2k_0^2}{4pk}L^+_\pi\right.\right.$$
$$+\frac{\omega_\pi k_0(2\eta_1^2p^2k_0^2-\eta_1\eta_2(k_0^2-k^2+m_\pi^2)}{4pk}L^-_\pi$$
$$+\frac{1}{2}k_0^2[2\eta_1^2(2p^2+m_\pi^2)-\eta_1\eta_2(k_0^2-k^2+m_\pi^2)]\Lambda^+_{p1}$$
$$\left.+\frac{1}{2}\omega_\pi k_0[\eta_1^2(k_0^2-k^2+m_\pi^2)-2\eta_1\eta_2(k_0^2+k^2)]\Lambda^-_{p1}+(\eta_1^2\omega_\pi k_0-\eta_1\eta_2k_0^2)\Lambda^-_{p2}\right]$$
$$+\frac{n(\omega_\rho)}{\omega_\rho}\left[\frac{\eta_1^2m_\rho^2k_0^2p^2}{4pk}L^+_\rho-\frac{m_\rho^2k_0\omega_\rho k^2(\eta_1^2-\eta_1\eta_2)}{4pk}L^-_\rho+\frac{1}{2}k_0^2m_\rho^2(2\eta_1^2-\eta_1\eta_2)\Lambda^+_{r1}\right.$$
$$\left.\left.+\frac{1}{2}\eta_1^2k_0\omega_\rho(m_\rho^2-2k^2)\Lambda^-_{r1}\right]\right\}, \tag{D2}$$

$$\Pi_{00}^{A_1} = -g^2 \int \frac{p^2 dp}{(2\pi)^2} \left\{ \frac{n(\omega_\pi)}{2\omega_\pi} \left[-4(\zeta_1 - \zeta_2 p^2 - \zeta_3 k^2) - \frac{\omega_\pi k_0^2 (\eta_1^2 p^2 + \eta_2^2 k^2)}{pk} L_\pi^- \right.\right.$$
$$- \frac{\eta_1^2 p^2 (k_0^2 + m_\pi^2) - \eta_2^2 k^2 (k_0^2 - k^2 + \omega_\pi^2) + 2p^2 k^2}{2pk} L_\pi^+$$
$$- [\eta_1^2 p^2 + \eta_2^2 p^2 - \eta_1 \eta_2 (k_0^2 - k^2 + m_\pi^2)] \Lambda_{p1}^+$$
$$\left. + \frac{1}{2}(\eta_1 + \eta_2)^2 \Lambda_{p2}^+ + 2\eta_1 \eta_2 \omega_\pi k_0 \Lambda_{p1}^- \right]$$
$$\left. + \frac{n(\omega_\rho)}{2\omega_\rho} \left[- \frac{\eta_1^2 m_\rho^2 p^2 + \omega_\rho^2 k^2 (\eta_1 - \eta_2)^2}{4pk} L_\rho^+ + m_\rho^2 (\eta_1^2 - \eta_1 \eta_2) \Lambda_{r1}^+ + \frac{1}{2}(\eta_1 - \eta_2)^2 \Lambda_{r2}^+ \right] \right\}, \quad \text{(D3)}$$

$$\Pi_\mu^{\mu A_1} = g^2 \int \frac{p^2 dp}{(2\pi)^2} \left\{ \frac{n(\omega_\pi)}{2\omega_\pi} \left[-4[4\zeta_1 + 3\zeta_2 m_\pi^2 + 3\zeta_3 (k_0^2 - k^2)] + \frac{3[\eta_1^2 m_\pi^4 + \eta_2^2 (k_0^2 - k^2)^2] - 4\eta_1 \eta_2 k^2 (k_0^2 - k^2)}{4pk} L_\pi^+ \right.\right.$$
$$+ \frac{(\eta_1^2 + \eta_2^2 + 4\eta_1 \eta_2)[m_\pi^2 (k_0^2 - k^2) + 2\omega_\pi^2 k_0^2]}{4pk} L_\pi^+$$
$$+ \frac{3\omega_\pi k_0 [\eta_1^2 m_\pi^2 + \eta_2^2 (k_0^2 - k^2) + \eta_1 \eta_2 (m_\pi^2 + k_0^2 - \frac{5}{3} k^2)]}{2pk} L_\pi^-$$
$$+ [3\eta_1^2 m_\pi^2 + 3\eta_2^2 (k_0^2 - k^2) + \eta_1 \eta_2 (3m_\pi^2 - 2k_0^2)] \Lambda_{p1}^+$$
$$\left. + 2k_0 \omega_\pi (\eta_1^2 + \eta_2^2 + 3\eta_1 \eta_2) \Lambda_{p1}^- + (\eta_1 + \eta_2)^2 \Lambda_{p2}^+ \right]$$
$$+ \frac{n(\omega_\rho)}{2\omega_\rho} \left[\frac{3\eta_1^2 m_\rho^4 + (\eta_1 - \eta_2)^2 [m_\rho^2 (k_0^2 - k^2) + 2\omega_\rho^2 k_0^2]}{4pk} + \frac{3(\eta_1^2 - \eta_1 \eta_2) \omega_\pi k_0 m_\rho^2}{2pk} L_\rho^- \right.$$
$$\left. \left. + 3(\eta_1^2 - \eta_1 \eta_2) m_\rho^2 \Lambda_{r1}^+ + 2(\eta_1 - \eta_2)^2 k_0 \omega_\rho \Lambda_{r1}^- + (\eta_1 - \eta_2)^2 \Lambda_{r2}^+ \right] \right\}, \quad \text{(D4)}$$

where

$$\zeta_1 = \frac{m_{A_1}^2}{m_\rho^2},$$
$$\zeta_2 = \frac{g^2 F_\pi^2}{8m_\rho^4} \left(\frac{1-\sigma}{1+\sigma} \right) + \frac{2g\xi}{1+\sigma} \frac{Z^2 \sqrt{1-\sigma}}{m_\rho^2},$$
$$\zeta_3 = \frac{4\sigma}{1+\sigma} \frac{1}{g^2 F_\pi^2},$$
$$L_\pi^\pm = L^\pm(\omega = \omega_\pi,\ m^2 = m_\pi^2 - m_\rho^2),$$
$$L_\rho^\pm = L^\pm(\omega = \omega_\rho,\ m^2 = m_\rho^2 - m_\pi^2),$$
$$\Lambda_{p,n}^\pm = \Lambda_n^\pm(\omega = \omega_\pi,\ m^2 = m_\pi^2 - m_\rho^2),$$
$$\Lambda_{r,n}^\pm = \Lambda_n^\pm(\omega = \omega_\rho,\ m^2 = m_\rho^2 - m_\pi^2). \quad \text{(D5)}$$

[1] J. I. Kapusta, *Finite Temperature Field Theory* (Cambridge University Press, Cambridge, England, 1989).
[2] E. V. Shuryak, Phys. Rep. **61**, 71 (1980).
[3] L. McLerran, Rev. Mod. Phys. **58**, 1021 (1986).
[4] E. V. Shuryak, Phys. Lett. **107B**, 103 (1981).
[5] R. D. Pisarski, Phys. Lett. **110B**, 155 (1982).
[6] C. DeTar, Phys. Rev. D **32**, 276 (1985); C. DeTar and J. Kogut, *ibid.* **36**, 2828 (1987).
[7] S. Gottlieb *et al.*, Phys. Rev. Lett. **59**, 347 (1987).
[8] M. Dey, V. L. Eletsky, and B. L. Ioffe, Phys. Lett. B **252**, 620 (1990).
[9] R. J. Furnstahl, T. Hatsuda, and Su H. Lee, Phys. Rev. D **42**, 1744 (1990); T. Hatsuda, Y. Koike, and Su H. Lee, Nucl. Phys. **B394**, 221 (1993); Phys. Rev. D **47**, 1225 (1993).
[10] C. Gale and J. Kapusta, Nucl. Phys. **B357**, 65 (1991).
[11] G. E. Brown and M. Rho, Phys. Rev. Lett. **66**, 2720 (1991).
[12] A. V. Smilga, Nucl. Phys. **B335**, 569 (1990).
[13] B. W. Lee and H. T. Nieh, Phys. Rev. **166**, 1507 (1968).

[14] J. I. Kapusta, in *Trends in Theoretical Physics*, edited by P. Ellis and Y. C. Tang (Addison-Wesley, Redwood City, CA, 1991); Vol. 2; E. V. Shuryak, Nucl. Phys. **A533**, 761 (1991).
[15] A. A. Abrikosov, L. P. Gorkov, and I. E. Dzyaloshinski, *Methods of Quantum Field Theory in Statistical Physics* (Dover, New York, 1963).
[16] E. Witten, Nucl. Phys. **B223**, 432 (1983).
[17] Ö. Kaymakcalan, S. Rajeev, and J. Schechter, Phys. Rev. D **30**, 594 (1984).
[18] J. Sakurai, *Current and Mesons* (University of Chicago Press, Chicago, 1969).
[19] B. W. Lee, *Chiral Dynamics* (Gordon and Breach, New York, 1972).
[20] S. Weinberg, Physica A **96**, 327 (1979).
[21] N. Knoll, T. D. Lee, and W. Zumino, Phys. Rev. **157**, 1376 (1967).
[22] S. Gasiorowicz and D. Geffen, Rev. Mod. Phys. **41**, 531 (1969).
[23] U.-G. Meissner, Phys. Rep. **161**, 213 (1988).
[24] R. Dashen, S. Ma, and J. Bernstein, Phys. Rev. **187**, 349 (1969).
[25] G. Welke, R. Venugopalan, and M. Prakash, Phys. Lett. B **245**, 137 (1990).
[26] H. Gomm, Ö. Kaymakcalan, and J. Schechter, Phys. Rev. D **30**, 2345 (1984).
[27] B. R. Holstein, Phys. Rev. D **33**, 3316 (1986).
[28] U.-G. Meissner and I. Zahed, Z. Phys. A **327**, 5 (1987).
[29] Chungsik Song, University of Minnesota Report No. NUC-MINN-93/2-T, 1993 (unpublished).
[30] Particle Data Group, K. Hikasa *et al.*, Phys. Rev. D **45**, S1 (1992).
[31] V. Eletsky, P. Ellis, and J. Kapusta, Phys. Rev. D **47**, 4084 (1993).
[32] K. Kajantie and J. Kapusta, Ann. Phys. (N.Y.) **160**, 477 (1985).
[33] U. Heinz, K. Kajantie, and T. Toimela, Ann. Phys. (N.Y.) **176**, 218 (1987).
[34] J. I. Kapusta, Phys. Rev. D **46**, 4749 (1992).
[35] J. Polonyi *et al.*, Phys. Rev. Lett. **53**, 644 (1984).
[36] F. E. Close, *An Introduction to Quarks and Partons* (Academic, New York, 1979).